

## Particle and photon detection for a neutron radiative decay experiment

T.R. Gentile<sup>a,\*</sup>, M.S. Dewey<sup>a</sup>, H.P. Mumm<sup>a</sup>, J.S. Nico<sup>a</sup>, A.K. Thompson<sup>a</sup>, T.E. Chupp<sup>b</sup>,  
R.L. Cooper<sup>b</sup>, B.M. Fisher<sup>c</sup>, I. Kremisky<sup>c</sup>, F.E. Wietfeldt<sup>c</sup>, K.G. Kiriluk<sup>d</sup>, E.J. Beise<sup>d</sup>

<sup>a</sup>National Institute of Standards and Technology, Gaithersburg, MD 20899, USA

<sup>b</sup>University of Michigan, Ann Arbor, MI 48109, USA

<sup>c</sup>Tulane University, New Orleans, LA 70118, USA

<sup>d</sup>University of Maryland, College Park, MD 20742, USA

Available online 11 April 2007

### Abstract

We present the particle and photon detection methods employed in a program to observe neutron radiative beta-decay. The experiment is located at the NG-6 beam line at the National Institute of Standards and Technology Center for Neutron Research. Electrons and protons are guided by a 4.6 T magnetic field and detected by a silicon surface barrier detector. Photons with energies between 15 and 750 keV are registered by a detector consisting of a bismuth germanate scintillator coupled to a large area avalanche photodiode. The photon detector operates at a temperature near 80 K in the bore of a superconducting magnet. We discuss CsI as an alternative scintillator, and avalanche photodiodes for direct detection of photons in the 0.1–10 keV range.

© 2007 Elsevier B.V. All rights reserved.

PACS: 29.30.Ep; 29.40.Mc

Keywords: Gamma-ray; Neutron decay; Photodiode; Radiative; Scintillator

In neutron beta-decay, a photon is emitted along with the proton, electron and antineutrino [1,2]. Despite decades of study, these inner-bremsstrahlung photons have yet to be definitively observed [3,4]. An experiment is in progress on the NG-6 fundamental physics beam line [5] at the National Institute of Standards and Technology Center for Neutron Research (NCNR) to measure the branching ratio for this process [6]. The radiation accompanying neutron decay is primarily due to inner bremsstrahlung from the electron and thus has a continuous spectrum with spectral intensity that decreases monotonically with increasing photon energy. High energy resolution is not a requirement for the photon detector, but large area is essential because the branching ratio is only  $\approx 3 \times 10^{-3}$  for photons above our detection threshold of 15 keV. Since the neutron lifetime is about 15 min, the detected rate for such photons is low ( $\approx 0.05 \text{ s}^{-1}$  for the experiment discussed in

this paper). To maximize the solid angle for electron and proton detection, these particles are guided to a single surface barrier detector (SBD) by a strong magnetic field from a superconducting solenoidal magnet. This design requires either a photon detector that operates in the 4.6 T magnetic field and near a temperature of 80 K, or a light guide to direct the light to a remote photon detector located in low field. We have chosen the former approach, and in this paper we describe a photon detector for energies between 15 and 750 keV that meets these requirements. It is based on a pure, inorganic scintillator coupled to a large area avalanche photodiode (APD) detector. We have also investigated the use of APDs to directly detect photons in the 0.1–10 keV range, for which the branching ratio is similar to that of the 15–750 keV range, due to the infrared divergent nature of neutron radiative decay.

The spectrometer for electron and proton detection consists of a superconducting solenoid with a slight bend at the upstream end. Charged particles emitted are trapped in helical orbits and those emitted in the upstream hemisphere drift toward a 600 mm<sup>2</sup> by 1 mm thick SBD [7]. The SBD is

\*Corresponding author.

E-mail addresses: [thomas.gentile@nist.gov](mailto:thomas.gentile@nist.gov) (T.R. Gentile),  
[cooperrl@umich.edu](mailto:cooperrl@umich.edu) (R.L. Cooper).

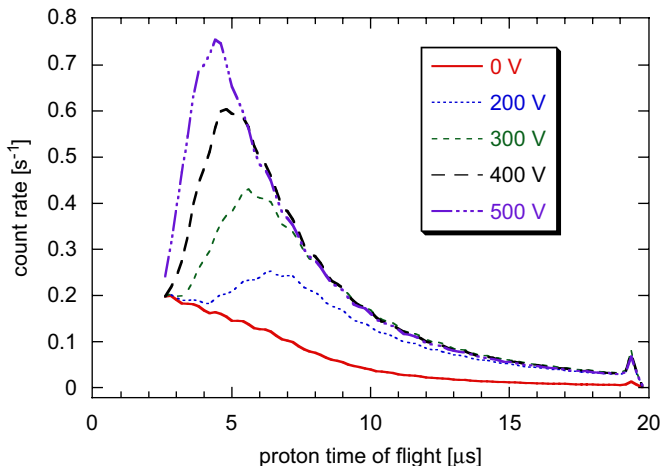


Fig. 1. Timing spectrum for the arrival of protons at the SBD with respect to the trigger from the much larger electron signal, shown for the accepted time window of 2.5–20 μs for five mirror voltages: 0 V (solid line); 200 V (dotted line); 300 V (short dashed line); 400 V (long dashed line); and 500 V (dot-dash line).

biased to –25 kV to accelerate the protons, which have initial energies less than 750 eV, so that they pass through the 40 μg/cm<sup>2</sup> gold entrance window. The maximum electron energy is 750 keV, hence most electrons easily penetrate the potential barrier. To greatly suppress the photon background associated with the neutron beam, we require that a trigger from a detected electron is followed by detection of a proton within the drift time expected for the relatively slow proton. In neutron decay, the direction of the electron and proton momenta are highly anticorrelated, hence an electrostatic mirror is used to reverse the protons emitted into the downstream hemisphere. Fig. 1 shows the spectrum for the arrival of protons at the SBD with respect to the (much larger) electron signal. Spectra are shown for five mirror voltages, illustrating the increase in the number of protons detected and a decrease in the average time delay as higher energy protons are reversed.

Scintillating crystals allow for a large solid angle of photon detection at relatively modest cost. APDs can efficiently detect the scintillation light and are insensitive to magnetic fields of a few Tesla [8]. Although the signal-to-noise ratio (S/N) for APDs is worse than that of photomultiplier tubes, it can be improved dramatically by cooling to 80 K [9]. Whereas doped inorganic crystals generally exhibit lower light yield at 80 K relative to room temperature [10], the yield from pure inorganic crystals increases at low temperature [11,12]. Fig. 2 shows the performance of a detector consisting of a 1.2 cm by 1.2 cm by 20 cm long bismuth germanate (BGO) crystal [13] in direct contact with a 1.35 cm by 1.35 cm APD [14] that was operated at a bias of 1378 V (≈ 20 V below breakdown). We found that to obtain a low threshold, it was critical for the APD to be as large or larger than the crystal face through which the scintillation light is coupled. The detector was located in the cold bore of a 4.6 T superconducting magnet and equilibrated at a temperature near

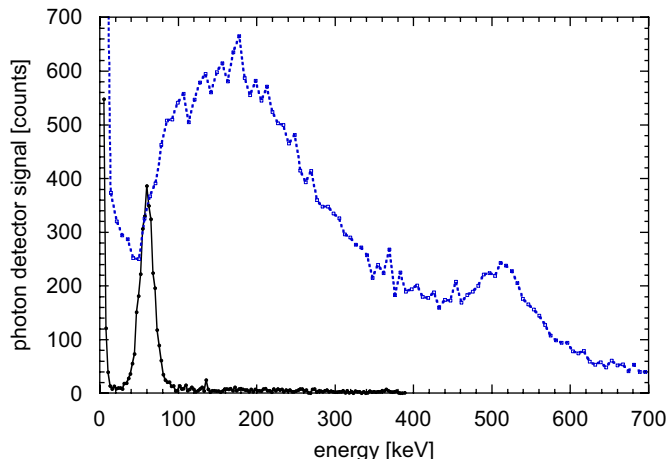


Fig. 2. Photon detector response for an <sup>241</sup>Am source (solid line) and the photon spectrum on the neutron beam line (dotted line).

80 K. The 60 keV gamma-ray from an <sup>241</sup>Am source was used to calibrate the energy scale. With the assumption of a linear response of the detector to photon energy with no offset, the detection threshold is 15 keV and the energy width of the 60 keV peak is 22 keV full width at half maximum (FWHM). The width is dominated by the statistics of electron-hole generation and multiplication in the APD [15]. The APD was connected to a preamplifier [16] and the waveform (without any pulse shaping) was registered by a digital oscilloscope card [17]. A single APD was employed for several months of operation and the gain was found to be quite stable. In Fig. 2 the photon spectrum observed by the detector on the neutron beam line is also shown. The broad features at 160 and 511 keV, presumed to be due to backscattering of higher energy photons from the reactor [18] and pair production, respectively, were used as gain monitors. With occasional adjustments of a few volts on the APD bias, the gain was found to be stable to within 10%.

In Fig. 3, a typical candidate neutron radiative decay event is shown, characterized by an electron–photon coincidence followed by a delayed proton. (Further analysis is required to isolate true radiative decay events from possible sources of background.) Since the signal from an electron is much larger than that from a proton, a simple threshold can be employed to trigger on electrons. The pulse shape for the APD signal exhibits a slow rise due to the long scintillation time for BGO at 80 K. Using a software template for the form of the APD signal, we extract the time delay between the electron signal and the onset of the APD signal, and the amplitude of the APD signal. In Fig. 4 is shown a histogram of photon detector counts vs. electron–photon time delay, for events in which a delayed proton is also observed. Due to electronic delays, the peak from photons detected in coincidence with the electron appears near –1 μs. Isolation of the candidate radiative decay events requires subtraction of the comparable flat background visible in Fig. 4. From this perspective, the S/N could be improved if a faster rise

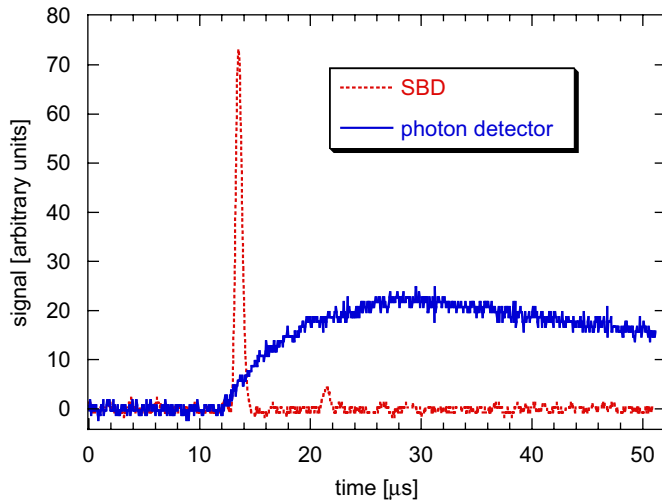


Fig. 3. A typical candidate neutron radiative decay event, shown as a function of time. The signals from the surface barrier detector (dotted line) for the electron (at  $\approx 14 \mu\text{s}$ ) and the delayed proton (at  $\approx 21 \mu\text{s}$ ) are shown, as well as the slow photon detector signal (solid line).

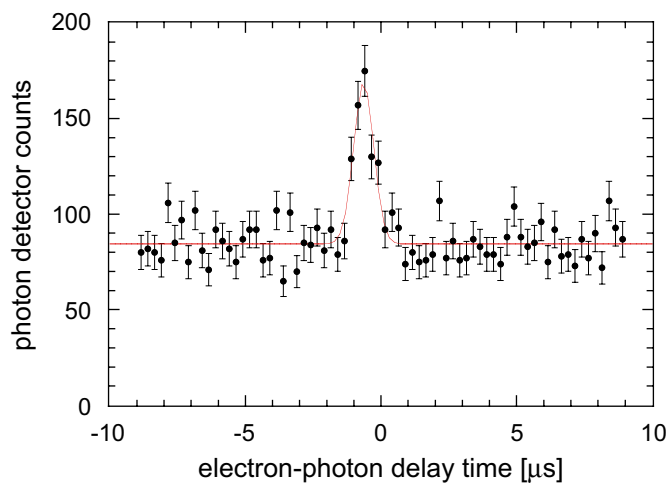


Fig. 4. Photon detector signal vs. electron-photon delay time, along with a fit to a Gaussian form.

time for the photon detector signal were possible. For this and other reasons, we are considering cesium iodide (CsI) as an alternative to BGO.

The potential advantage of CsI for this work is its  $1.0 \mu\text{s}$  scintillation decay time [12], which is about 5 times shorter than for BGO. Other parameters important for a comparison of the two crystals include light yield, scintillation wavelength range, crystal stability and associated effects, and response characteristics. Whereas the scintillation light yields at 300 K for BGO and CsI are 8 photons per keV [18] and 3.2 photons per keV [12], respectively, the expected increases in these yields upon cooling to 80 K are factors of 2.9 [11] and 15.8 [12], respectively. We found the light yield for CsI at 80 K to be equal to or better than that of BGO, but this comparison was complicated by an observed dependence of the CsI response to the spatial location along the 20 cm crystal. CsI

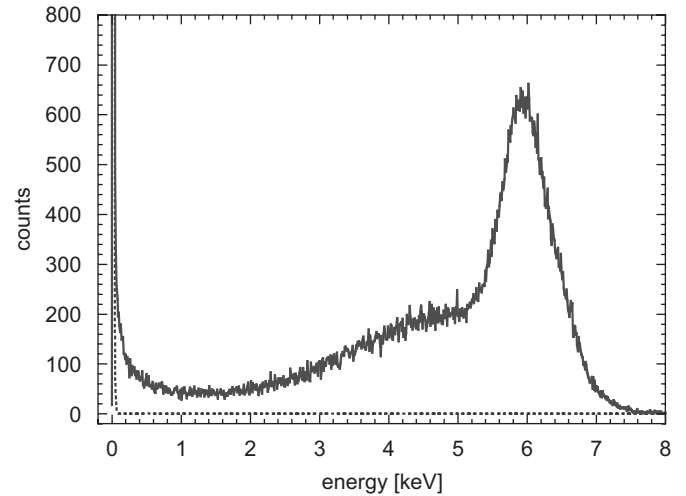


Fig. 5. Response of the APD to an  $^{55}\text{Fe}$  source. The solid and dotted lines shows the data obtained with the source in place and removed, respectively.

is weakly hygroscopic, and this large spatial dependence (50% of the maximum efficiency) appeared to be related to this issue. The spatial dependence was substantially reduced by sufficient repolishing of the crystal, but returned when the crystal was painted with a red fluorescent paint. (The effect of painting was reversible, i.e. by removing the paint with acetone we could recover the good spatial uniformity of the response observed before painting.) This paint was applied to increase the light detection efficiency by shifting the scintillation wavelength range from the near ultraviolet to the red, as well as to seal the surface from water absorption [12]. CsI also caused contamination of the APD surface, which is in direct contact with one face of the crystal. CsI has a substantially greater proportion of Compton scattering as compared to BGO, but this is not expected to be a serious issue in this experiment due to rapid decrease in higher energy photons in the expected spectrum for neutron radiative decay. We plan further studies to evaluate the use of CsI.

Finally, we consider APDs for direct detection of neutron radiative decay photons. In Fig. 5 the response of an APD to an  $^{55}\text{Fe}$  source is shown, as registered by a multichannel analyzer [19]. The APD was operated at a bias of 1525 V (45 V below breakdown) off the neutron beam line in a cryostat cooled with liquid nitrogen. The X-rays from the source entered the cryostat through a 0.13 mm thick polyimide window and two layers of 0.05 mm thick aluminized tape. The APD signal was sent to a preamplifier [16], followed by a pulse shaping amplifier set for a  $3 \mu\text{s}$  peaking time. (For direct detection, we found pulse shaping slightly better than linear amplification.) The 5.9 keV X-ray from the  $^{55}\text{Fe}$  source was used to calibrate the energy scale. With the assumption of a linear response of the APD to photon energy with no offset, we obtain a detection threshold of 0.1 keV and an energy width of 1.0 keV FWHM. The width is dominated by the statistics

of electron-hole generation and multiplication in the APD [15]. Above  $\approx 10$  keV, the detection efficiency decreases because the absorption length becomes longer than the thickness of the APD. Due to lower background in this energy range, as well as the much shorter rise time as compared to that obtained from scintillation, preliminary tests on the beam line indicate that the background apparent in Fig. 4 can be reduced by at least an order of magnitude. The largest drawback of this approach is the relatively small detection area per APD than that of the scintillator–APD combination. Nevertheless, we are considering the use of direct detection, as it would allow us to span two additional decades in photon energy.

In summary, we have presented the particle and photon detection methods for an experiment to observe neutron radiative decay. Electrons and protons are guided by a 4.6 T magnetic field and detected by a silicon surface barrier detector. We have operated a photon detector based on a BGO scintillator coupled to a large area APD in the cryogenic environment of a superconducting magnet for detection of 15–750 keV photons. We are currently developing a multichannel detector to increase the solid angle for photon detection by a factor of 12. The range of photon energies detected may also be extended down to 0.1 keV by direct detection with APDs.

We acknowledge useful conversations with R. Farrell and support from the Dept. of Energy and the National Science Foundation.

#### Note added in proof

During the publication process for this paper, we have observed the radiative decay mode of the neutron using the methods described in this paper; the results can be found in J.S. Nico et al, *Nature* 444, 1059–1062 (2006).

#### References

- [1] Yu.V. Gaponov, R.U. Khafizov, *Nucl. Instr. and Meth. A* 440 (2000) 557.
- [2] V. Bernard, S. Gardner, U.-G. Meiner, C. Zhang, *Phys. Lett. B* 593 (2004) 105;  
V. Bernard, S. Gardner, U.-G. Meiner, C. Zhang, *Phys. Lett. B* 599 (2004) 348.
- [3] M. Beck, et al., *JETP Lett.* 76 (2002) 392.
- [4] R.U. Khafizov, et al., *JETP Lett.* 83 (2006) 5. The results in this paper have recently been disputed in N. Severijns, et al., *nucl-ex/0607023*; *JETP Lett.* 84 (2006) 231.
- [5] J.S. Nico, et al., *J. Res. Natl. Inst. Stand. Technol.* 110 (2005) 137.
- [6] B.M. Fisher, et al., *J. Res. Natl. Inst. Stand. Technol.* 110 (2005) 421.
- [7] Advanced Measurement Technology, 801 S. Illinois Avenue, Oak Ridge, Tennessee 28260-1175. Certain trade names and company products are mentioned in the text or identified in an illustration in order to adequately specify the experimental procedure and equipment used. In no case does such identification imply recommendation or endorsement by the National Institute of Standards and Technology, nor does it imply that the products are necessarily the best available for the purpose.
- [8] M. Boucher, et al., *Nucl. Instr. and Meth.* 505 (2003) 136.
- [9] M. Moszynski, et al., *IEEE Trans. Nucl. Sci.* NS-49 (2002) 971;  
L. Yang, et al., *Nucl. Instr. and Meth. A* 508 (2003) 388.
- [10] (<http://www.detectors.saint-gobain.com/>).
- [11] H.V. Piltingsrud, *J. Nucl. Med.* 20 (1979) 1279.
- [12] C. Amsler, et al., *Nucl. Instr. and Meth. A* 480 (2002) 494.
- [13] Rexon Components, Inc., 24500 Highpoint Rd., Beachwood, Ohio 44122.
- [14] Radiation Monitoring Devices, Inc., Watertown, MA 02472.
- [15] M. Moszynski, M. Szawlowski, M. Kapusta, M. Balcerzyk, *Nucl. Instr. and Meth. A* 497 (2003) 226.
- [16] Canberra Model 2006 Proportional Counter Preamplifier, Canberra Industries, 800 Research Parkway, Meriden, Connecticut 06450.
- [17] Gage CompuScope 82G, DynamicSignals LLC, 900 N. State Street, Lockport, Illinois 60441.
- [18] G.F. Knoll, *Radiation Detection and Measurement*, Wiley, New York, 2000.
- [19] Quantum MCA8000, Princeton Gamma-Tech, Inc., C/N 863, Princeton, NJ 08542-0863.